Aqueous Manganese Dioxide Ink for High Performance Capacitive Energy Storage Devices

Jiasheng Qian, Shu Ping Lau and Jikang Yuan

Department of Applied Physics, the Hong Kong Polytechnic University, Hong Kong SAR

ABSTRACT:

We report a simple approach to fabricate high performance energy storage devices based on aqueous inorganic ink comprised of hexagonal MnO_2 nanosheets. The MnO_2 ink exhibits long term stability. Continuous thin films can be formed on various substrates without using any binder. To obtain a flexible electrode for capacitive energy storage, we printed the MnO_2 ink on commercially available A4 paper pre-treated by multi-walled carbon nanotubes. The electrode exhibited a maximum specific capacitance of 90.8 mF/cm^2. The electrode could maintain 98.7% capacitance retention for 1,000 cycles at 10 mV/s. The MnO_2 ink could be a potential candidate for large-scale production of flexible and printable electronic devices for energy storage and conversion.

INTRODUCTION:

Printable electronics has been paid much attentions in the past few years due to its potential applications ranging from thin film transistors (TFTs), energy storage devices, solar cells to wearable devices [1-4]. Preparations of various inks composed of semiconductors, insulators, and carbon materials have been reported [5-7], attracting much attention because they are inexpensive with combination of wide printability on different substrates and suitable for mass production in industry. By virtue of abundance, high theoretical energy capacity and environmental compatibility, manganese dioxide is usually regarded as an ideal candidate for the electrode materials of portable devices, water treatment, up-conversion as well as photocatalysis. The conventional MnO_2 electrodes are mainly prepared by two approaches: (1) nanostructured MnO_2 or MnO_2-containing composite precipitates *via* wet chemical processes [8, 9]; (2) direct electrodeposition or chemical deposition on various substrates (e.g. glass, quartz, copper or aluminum foil) [10, 11]. These existing preparation methods suffer from higher cost, complicated processes and superfluous contaminations. By now, it still remains a great challenge to synthesize MnO_2 inks with high reliability and versatility. Nevertheless, few research works in this field have been reported to date [12, 13].

EXPERIMENT:

Preparation of the MnO_2 ink.

All chemicals were analytical reagents purchased from International Laboratory USA and were used without further purification. The aqueous MnO_2 ink was prepared according to the previous report with some modifications [14]. Typically, 10wt% glucose solution was prepared

by dissolving 1 g glucose (A.R.) into 10 ml deionized (DI) water and treated by microwave hydrothermal process at 350 psi and 300 °C for 10 min to obtain highly crystalline carbon particles (HCCPs). When the reaction was completed, the solution was poured out for filtration (filter membrane, ø: 220μm). 10 mg HCCPs residues were re-dissolved into 100 mL DI water and sonicated sufficiently to form HCCPs suspension. Then 80 mg $KMnO_4$ (A.R.) was dissolved into 5 mL DI water and added into the HCCPs suspension dropwise under continuous stirring and maintained at room temperature for 48h. It is suggested that the reaction proceeds as follows:

$$4MnO_4^- + 3C + H_2O \rightarrow 4MnO_2 + CO_3^{2-} + 2HCO_3^-$$

When the reaction was completed, the resultant solution was filtered by using filter paper to remove the excess reactants. Subsequently, the pH value of the solution was adjusted to neutral by dialysis (Thermo Scientific, 3.5K MWCO). Finally, ~1 mg/mL MnO_2 ink was obtained.

Characterization instruments.

The microstructure of MnO_2 ink were characterized by JEM 2100F (field emission) scanning transmission electron microscope (TEM). The morphology of MnO2@conductive paper was recorded by using atomic force microscope (AFM, Digital Instrumental Nanoscope IV) in tapping mode. Sheet resistance of the conductive paper was measured by a four-point probe system at room temperature.

Electrode and capacitor construction.

For the preparation of the MnO_2@conductive paper electrode, commercial A4 paper (Double A) was pre-treated by multi-walled carbon nanotubes (MCNTs, commercial product) with 0.5, 0.8, 1.0 and 1.2 mg/cm^2 (denoted as P-0.5, P-0.8, P-1 and P-1.2), respectively, to form the conductive paper. Then 1 mg/mL MnO_2 ink was deposited with aid of surfactant (sodium dodecylbenzenesulfonate, SDBS) on as-prepared conductive paper by 80 μg/cm^2, and then washed thoroughly by DI water to remove the surfactant. For the electrochemical measurements, a 1.5×1 cm paper electrode was applied. To reduce the resistance between alligator clip and electrode, 0.5×1 cm of paper electrode was erased by 1 mol/L oxalic acid solution to remove the MnO_2 and then coated by silver paint.

Electrochemical measurements.

All the electrochemical experiments were performed at ambient temperature. A three-electrode system was applied by using paper electrode as the working electrode, platinum electrode as the counter electrode and Ag/AgCl electrode as the reference electrode. All the cyclic voltammograms (CV), galvanostatic charge-discharge (GCD) and electrochemical impedance spectrum (EIS) measurements were carried out on a CHI 660C electrochemical workstation (CH Instruments). The specific areal and gravimetric capacitance (C_{sp}, mF/cm^2) were calculated according to the following equations (1):

$$C_{sp} = \frac{\Delta Q}{2 \times \Delta V \times S \times r} \quad (1)$$

where ΔQ is the charge integrated from the whole voltage range; ΔV is the whole range of

voltage window; S is the total area of active material on the electrodes; r is the scan rate of CV measurement.

The GCD measurements at various current densities were performed. Specific areal and gravimetric capacitance (C_{sp}, mF/cm^2) of each electrode were calculated according to the equations (2):

$$C_{\mathrm{sp}} = \frac{I \times \Delta t}{\Delta V \times S} \tag{2}$$

where I is the discharge current; Δt is the discharge time; ΔV is the voltage difference within the discharge time Δt; S is the total area of active material on the electrodes.

DISCUSSION:

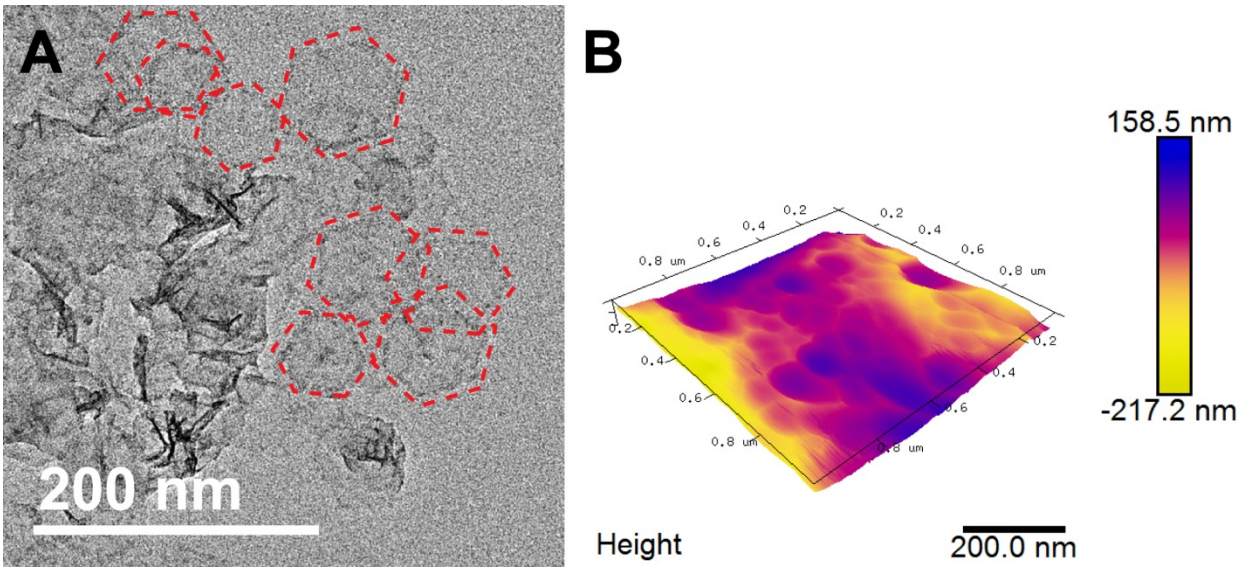

Figure 1. The morphology of MnO_2 ink and MnO_2 thin films. A) TEM image of hexagonal MnO_2 nanosheets with <100 nm in diameter. B) 3D model image of MnO_2@conductive paper electrode (P-0.8) measured by AFM.

High resolution TEM image of MnO_2 ink was shown in Figure 1A, which revealed the MnO_2 ink is comprised of hexagonal MnO_2 nanosheets (*h*-MnNSs) with a diameter less than 100 nm. Furthermore, clear edges of the nanosheets could be observed along with the red dash lines. The conductive paper was prepared by coating different amount of multi-walled carbon nanotubes (MCNTs) on the commercial A4 paper. The mass loading of MCNTs was controlled in 0.5, 0.8, 1.0 and 1.2 mg/cm^2, respectively, which are denoted as P-0.5, P-0.8, P-1.0 and P-1.2. According to our previously report, the optimized mass loading of MnO_2 ink could be 80 μg/cm^2. After the MnO_2 ink was coated onto the conductive paper, the thickness and roughness of the MnO_2@conductive paper could be investigated by the AFM image, which is shown in Figure 1B. The maximum height difference could be ~380nm, indicating a compact thin film that combined MnO_2 and MCNTs coated on the paper. This kind of MnO_2@MCNTs networks could provide a high electrical conductivity, resulting in an enhanced specific capacitance.

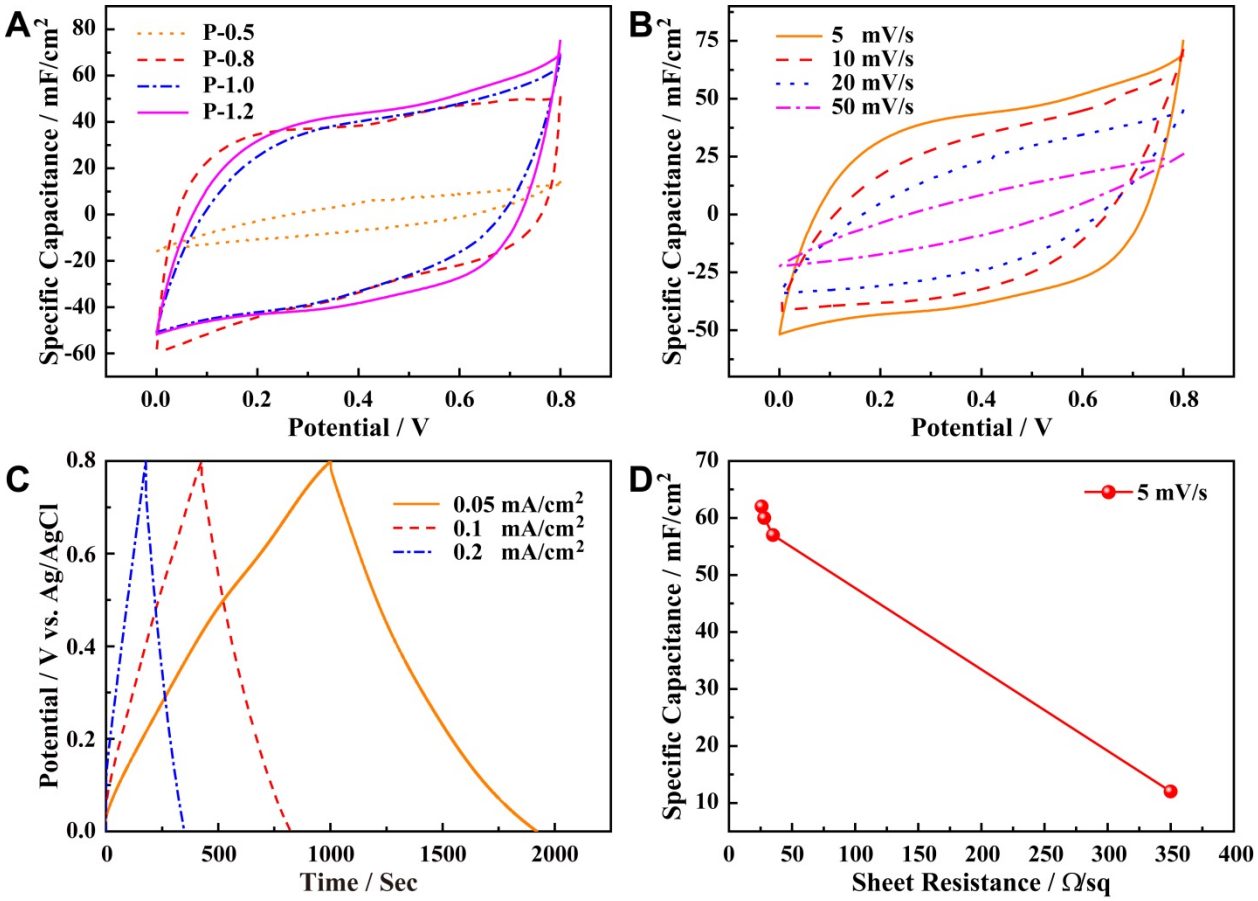

Figure 2. Electrochemical performances of MnO_2@conductive paper electrodes. A) CV curves of the MnO_2@conductive paper electrodes with different mass loadings of MCNTs at 5 mV/s. B) CV curves of the P-1.2 paper electrodes at different scan rates of 5, 10, 20 and 50 mV/s, respectively. C) GCD curves of the P-1.2 paper electrode at different current densities of 0.05, 0.1 and 0.2 mA/cm^2, respectively. D) Specific capacitance versus sheet resistance of the paper electrodes. The specific capacitances are estimated from the CV curves at 5 mV/s.

The cyclic voltammetry (CV) curves of different MnO_2@conductive paper electrodes at 5 mV/s are shown in Figure 2A, which all exhibits rectangular-like shapes. Such shapes are attributed to high speed ion-transport on electrode/electrolyte interface with rapid charging and discharging characteristics that is based on a redox reaction as follows (Equation 3) [15]:

$$MnO_2 + xH^+ + yNa^+ + (x+y)e^- \leftrightarrow MnOOH_xNa_y \quad (3)$$

Notably, the calculated specific capacitance of P-1.2 paper electrode reached the highest value of 62 mF/cm^2 among all the samples at 5 mV/s, which is about 9 times higher than that of the pure MCNTs electrode (7.2 mF/cm^2). Such an enhanced performance is attributed to the conformal MnO_2 thin films that contribute huge pseudo-capacitance. The CV curves of P-1.2 paper electrodes at different scan rates are exhibited in Figure 2B. With the increasing of scan rate, the rectangular shape of CV curve could still maintain at 20 mV/s. A maximum specific capacitance

of 90.8 mF/cm^2 (1135 F/g) is achieved by P-1.2 paper electrode at 2 mV/s, which is about 10 times higher than that of pure MCNTs electrode (8.9 mF/cm^2) and this value is almost equal to or higher than those of the reported MnO_2 electrodes [16, 17], even approaching the theoretical value of 1370 F/g. When the scan rate reaches 50 mV/s, the specific capacitance of P-1.2 paper electrode still retains a reasonable value of 21 mF/cm^2. For the P-0.5 paper electrode, the specific capacitance could only reach 9.6 mF/cm^2 at a low scan rate of 5 mV/s due to the poor electrical conductivity caused by insufficient mass loading of MCNTs. Galvanostatic charge/discharge (GCD) characteristics of P-1.2 electrode are performed in harmony with the results of CV measurements, as shown in Figure 2C. Apparently, symmetric triangular shapes appeared in the GCD which also matches the CV curves in Figure 2B. Furthermore, when a current density of 0.2 mA/cm^2 was applied, the P-1.2 paper electrode could reach a capacitance value as high as 43 mF/cm^2, indicating a potential electrode for the applications of the high-power devices [18]. Specific capacitance versus sheet resistance of the paper electrodes is exhibited in Figure 2D. With the increasing of mass loading of MCNTs from 0.5 mg/cm^2 (P-0.5 paper electrode) to 1.2 mg/cm^2 (P-1.2 paper electrode), the specific capacitance increased from 12 to 62 mF/cm^2 due to the significant improvement of electrical conductivity. When the electrical conductivity was increased to 35 Ω/sq (P-0.8 paper electrode), very less increment of specific capacitance was measured and the values of specific capacitances of P-0.8, P-1.0 and P-1.2 paper electrodes are almost on the same level, indicating a sufficient conductivity was achieved.

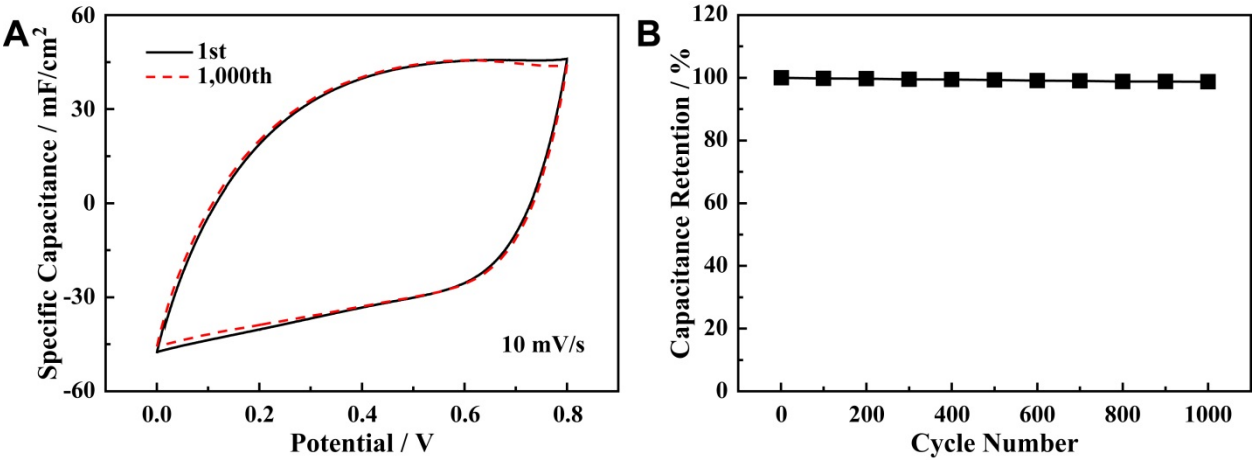

Figure 3. Cycle performances of P-1.2 paper electrode. A) CV curves of the first and the 1,000th cycle. B) 1,000 cycles capacitance retention versus cycle number.

As shown in Figure 3, the P-1.2 paper electrode underwent 1,000 cycles CV measurements at 10 mV/s. As a result, the CV shape could still remain the same and the specific capacitance retained 98.7%, revealing a prolonged lifetime.

CONCLUSIONS:

In summary, aqueous MnO_2 ink with long term stability and wide printability was prepared successfully. The electrochemical performances of MnO_2 coated paper electrode are exhibited

that achieved high specific capacitance and long term cycling performance. All these properties allow the MnO_2 ink to be an ideal candidate for large-scale production of high performance electronic devices in the near future.

ACKNOWLEDGEMENTS:

This work is supported in part by the Research Grants Council (RGC) of Hong Kong through the General Research Fund (Project no. PolyU 5292/12E and PolyU 153012/14P) and the Hong Kong Polytechnic University (Grant nos. 1-ZV5K and 1-ZV9B). We thank Dr. Chi Man Luk, Dr. Bolei Chen and Mr. Huanyu Jin for their assistance during the measurements.

REFERENCES:

1. J. Embden, A. S. R. Chesman, E. D. Gaspera, N. W. Duffy, S. E. Wathins and J. J. Jasieniak, *J. Am. Chem. Soc.* **136**, 5237 (2014).
2. D. Tobjörk and R. Österbacka, *Adv. Mater.* **23**, 1935 (2011).
3. K. K. Banger, Y. Yamashita, K. Mori, R. L. Peterson, T. Leedham, J. Rickard and H. Sirringhaus, *Nat. Mater.* **10**, 45 (2011).
4. J. A. Rogers and Y. G. Huang, *Proc. Natl. Acad. Sci., USA* **106**, 10875 (2009).
5. L. Hu, J. W. Choi, Y. Yang, S. Jeong, F. L. Mantia, L.-F. Cui and Y. Cui, *Proc. Natl. Acad. Sci., USA* **106**, 21490 (2009).
6. J. Wang, K. K. Manga, Q. Bao and K. P. Loh, *J. Am. Chem. Soc.* **133**, 8888 (2011).
7. J.-H. Choi, H. Wang, S. J. Oh, T. Paik, P. S. Jo, J. Sung, X. Ye, T. Zhao, B. T. Diroll, C. B. Murray and C. R. Kagan, *Science* **352**, 205 (2016).
8. Z. Fan, J. Yan, T. Wei, L. Zhi, G. Ning, T. Li and F. Wei, *Adv. Funct. Mater.* **21**, 2366 (2011).
9. M.-K. Song, S. Cheng, H. Chen, W. Qin, K.-W. Nam, S. Xu, X.-Q. Yang, A. Bongiorno, J. Lee, J. Bai, T. A. Tyson, J. Cho and M. Liu, *Nano Lett.* **12**, 3483 (2012).
10. X. Lu, M. Yu, G. Wang, T. Zhai, S. Xie, Y. Ling, Y. Tong and Y. Li, *Adv. Mater.* **25**, 267 (2013).
11. G. Yu, L. Hu, N. Liu, H. Wang, M. Vosgueritchian, Y. Yang, Y. Cui and Z. Bao, *Nano Lett.* **11**, 4438 (2011).
12. Z. Wang, R. Winslow, D. Madan, P. K. Wright, J. W. Evans, M. Keif and X. Rong, *J. Power Sources* **268**, 246 (2014).
13. L. Coustan, A. L. Comte, T. Brousse and F. Favier, *Electrochim. Acta* **152**, 520 (2015).
14. J. Qian, H. Jin, B. Chen, M. Lin, W. Lu, W. M. Tang, W. Xiong, L. W. H. Chan, S. P. Lau and J. Yuan, *Angew. Chem. Int. Ed.* **54**, 6800 (2015).
15. J. Qian, M. Liu, L. Gan, P. K. Tripathi, D. Zhu, Z. Xu, Z. Hao, L. Chen and D. S. Wright, *Chem. Commun.* **49**, 3043 (2013).
16. Z.; Su, C.; Yang, B. Xie, Z. Lin, Z. Zhang, J. Liu, B. Li, F. Kang and C. P. Wong, *Energy Environ. Sci.* **7**, 2652 (2014).
17. H. Jiang, T. Sun, C. Li and J. Ma, *J. Mater. Chem.* **22**, 2751 (2012).
18. D.-W. Wang, F. Li, M. Liu, G. Q. Lu and H.-M. Cheng, *Angew. Chem. Int. Ed.* **47**, 373 (2008).